



# A carbon cycling model shows strong control of seasonality and importance of sponges on the functioning of a northern Red Sea coral reef

Nanne van Hoytema<sup>1</sup> · Jasper M. de Goeij<sup>2</sup> · Niklas A. Kornder<sup>2</sup> · Yusuf El-Khaled<sup>3,4</sup> · Dick van Oevelen<sup>5</sup> · Laura Rix<sup>6</sup> · Ulisse Cardini<sup>7</sup> · Vanessa N. Bednarz<sup>8</sup> · Malik S. Naumann<sup>10</sup> · Fuad A. Al-Horani<sup>9,11</sup> · Christian Wild<sup>3</sup>

Received: 5 August 2022 / Accepted: 19 December 2022  
© The Author(s) 2023, corrected publication 2023

**Abstract** Coral reefs in the northern Red Sea experience strong seasonality. This affects reef carbon (C) cycling, but ecosystem-wide quantification of C fluxes in such reefs is limited. This study quantified seasonal reef community C fluxes with incubations. Resulting data were then incorporated into seasonal linear inverse models (LIM). For spring, additional sponge incubation results allowed for unique assessment of the contribution of sponges to C cycling. The coral reef ecosystem was heterotrophic throughout all seasons as gross community primary production (GPP; 136–200, range of seasonal means in  $\text{mmol C m}^{-2} \text{d}^{-1}$ ) was less than community respiration (R; 192–279), and balanced by

import of organic carbon (52–100), 88–92% of which being dissolved organic carbon (DOC). Hard coral GPP (74–110) and R (100–137), as well as pelagic bacteria DOC uptake (58–101) and R (42–86), were the largest C fluxes across seasons. The ecosystem was least heterotrophic in spring (highest irradiance) (GPP:R 0.81), but most heterotrophic in summer and fall with higher water temperatures (0.68 and 0.60, respectively). Adding the sponge community to the model increased community R ( $247 \pm 8$  without to  $353 \pm 13$  with sponges (mean  $\pm$  SD)). Sponges balanced this demand primarily with DOC uptake ( $105 \pm 6$ , 97% by cryptic sponges). This rate is comparable to the uptake of DOC by pelagic bacteria ( $104 \pm 5$ ) placing the cryptic sponges among the dominant C cycling groups in the reef.

Nanne van Hoytema and Jasper M. de Goeij have contributed equally to this work.

**Supplementary Information** The online version contains supplementary material available at <https://doi.org/10.1007/s00338-022-02339-3>.

✉ Jasper M. de Goeij  
j.m.degoeij@uva.nl

<sup>1</sup> Arcadis Nederland B.V, Beaulieustraat 22, 6814 DV Arnhem, The Netherlands

<sup>2</sup> Department of Freshwater and Marine Ecology, Institute for Biodiversity and Ecosystem Dynamics, University of Amsterdam, P.O. Box 94248, 1090 GE Amsterdam, The Netherlands

<sup>3</sup> Marine Ecology Department, Faculty of Biology and Chemistry, University of Bremen, Bremen, Germany

<sup>4</sup> Division of Biological and Environmental Science and Engineering (BESE), Red Sea Research Center (RSRC), King Abdullah University of Science and Technology (KAUST), Thuwal, Saudi Arabia

<sup>5</sup> Department of Estuarine and Delta Systems, Royal Netherlands Institute for Sea Research (NIOZ), Yerseke, The Netherlands

**Keywords** Coral reef ecosystem metabolism · LIM food web model · Red Sea · Primary production · Cryptic habitat · Sponge loop

<sup>6</sup> School of Chemistry and Molecular Biosciences, Australian Centre for Ecogenomics, University of Queensland, St. Lucia, QLD 4072, Australia

<sup>7</sup> Department of Integrative Marine Ecology (EMI), Stazione Zoologica Anton Dohrn – National Institute of Marine Biology, Ecology and Biotechnology, Genoa Marine Centre, Genoa, Italy

<sup>8</sup> Federal Office for Radiation Protection, Ingolstädter Landstraße 1, 85764 Oberschleißheim, Germany

<sup>9</sup> School of Basic and Marine Sciences, The University of Jordan, Aqaba Branch, P.O. Box 2595, Aqaba 77110, Jordan

<sup>10</sup> MARUM - Center for Marine Environmental Sciences, University of Bremen, Bremen, Germany

<sup>11</sup> School of Basic and Marine Sciences, The University of Jordan, Aqaba Branch, Aqaba, Jordan

## Introduction

Warm-water coral reefs thrive under oligotrophic conditions (Odum and Odum 1955; Webb et al. 1975; Kleypas et al. 1999) and maintain high gross primary production (GPP) due to efficient utilization and recycling of nutrients and organic matter (e.g., Wild et al. 2004; de Goeij et al. 2013). This high productivity allows coral reefs to provide ecosystem services to close to a billion people living on their shores (Sing Wong et al. 2022). To protect these valuable services, it is important to understand the elemental cycles (e.g., carbon; C) supporting them.

Coral reefs in the northern Red Sea experience higher seasonal variation in light availability and water temperature compared to most other warm-water coral reefs due to their occurrence at relatively high latitude (29° N). The stratified summer conditions and deep-water mixing in winter create strongly oligotrophic conditions and higher inorganic nutrient concentrations, respectively (Silverman et al. 2007; Rasheed et al. 2012; Carlson et al. 2014). The annual variation in environmental conditions makes the northern Red Sea an ideal natural laboratory to investigate effects of such variation on key coral reef ecosystem functions, such as C cycling (Berumen et al. 2019).

Trophic food web models have been developed for many coral reefs to explore C-cycling through ecosystems (e.g., Johnson et al. 1995; Niquil et al. 1998; Varkey et al. 2012; Heymans et al. 2014), but most have focused on fisheries aspects and therefore on the top of the food web. To our knowledge, only one such fisheries model exists for a Red Sea reef (Tsehaye and Nagelkerke 2008). Additionally, bottom-up trophic models for coral reefs—i.e., C cycling through benthic and pelagic primary producers and import of C from the open ocean—are largely lacking. Trophic models are often based on a combination of field data and estimates from literature with varying levels of uncertainty on the studied system. Linear inverse trophic models allow incorporation of these uncertainties into the model by entering data as ranges (Vézina and Platt 1988; Soetaert and van Oevelen 2009). Uncertainties can then be transferred to the model results by an iterative solution method. In this way, the model output reflects the quality of various types of input data in relation to the studied system. Additionally, linear inverse models can cope with data gaps. This makes linear inverse models well suited for resolving C cycling in complex systems, such as coral reefs.

In this study, we applied linear inverse modeling to study C fluxes on a northern Red Sea coral reef during four seasons. In one season (spring), we included the role of sponges, a less-studied component of the benthic community, in reef C cycling. Sponges take up large amounts of organic C, predominantly dissolved organic carbon (DOC) (e.g., Yahel et al. 2003; de Goeij et al. 2008; Hoer et al. 2018; Wooster

et al. 2019) at rates close to gross primary production rates of an entire coral reef ecosystem (de Goeij et al. 2013). Through the so-called sponge loop (de Goeij et al. 2013), sponges release particulate organic carbon (Alexander et al. 2014; Maldonado 2016; Rix et al. 2016; Kornder et al. 2022) and shunt it to higher trophic levels (Rix et al. 2018; Bart et al. 2021). Recently, an alternative penultimate pathway for the sponge loop has been hypothesized for sponges with massive growth, which do not release particulate organic carbon, but produce biomass that feeds sponge predators (McMurray et al. 2018; Pawlik and McMurray 2020). One of the reasons sponges are less studied in terms of C cycling is that a large part of the sponge community is generally overlooked by standard survey techniques (Kornder et al. 2021; Vicente et al. 2021). They are “hidden” within the three-dimensional framework of reefs—the cryptic habitat—considered the largest and least explored habitat of coral reefs (Richter et al. 2001; de Goeij and van Duyl 2007). The reef under study here is one of the few locations where the extent (e.g., volume and surface area) of the reef’s cryptic habitat and its community composition have been thoroughly studied, although two decades ago (Richter et al. 2001). Richter et al. (2001) used an endoscopic camera system to explore cavities up to 4 m into the reef structure. They found for the study area that each planar m<sup>2</sup> of reef harbors up to 7.5 m<sup>2</sup> of cryptic surface area. Further, sponges constituted 51–73% of live cover in the cryptic habitat. Combining these data, Richter et al. (2001) calculated an average cryptic sponge surface cover of 0.82 m<sup>2</sup> per planar m<sup>2</sup> of reef. However, the potential role of sponges in C cycling at the ecosystem scale has never been established for Red Sea reefs.

The models for the four seasons and the model in spring including the sponge community were fed with data from incubation measurements of the most important functional groups. These incubations measured the major C-cycling processes such as primary production, respiration, uptake, and release of organic C. The model design focused specifically on the bottom (i.e., benthic reef communities) of the food web, which is often simplified in other models. Compartments such as reef fish were not added in this model as data were lacking for these compartments in the study area.

## Material and methods

The models presented here are based on a large amount of data from various methods. Full descriptions of these methods can be found in the online resource. To keep this section concise and focused on how the models were developed, only brief descriptions of the field measurements and incubation methods are presented here.

## Study site and environmental monitoring

The field work for this study was conducted on the fringing coral reef adjacent to the Marine Science Station (MSS) of the University of Jordan and Yarmouk University, Aqaba, Jordan (29°27'31" N, 34°58'26" E). All sampling and monitoring were performed on the reef at 10 m water depth during four 28-d study periods in February, April, September, and November 2013. The timing of these periods (hereafter called winter, spring, summer, and fall, respectively) was previously determined from literature to best cover the annual cycle of key environmental parameters in the Gulf of Aqaba (Silverman et al. 2007; Carlson et al. 2014). The variation in light and temperature regime was monitored continuously with Onset HOBO data loggers (Pendant UA-002-64; temperature accuracy:  $\pm 0.53$  °C, spectral detection range: 150–1200 nm). Simultaneous measurements with Onset HOBO data loggers and a quantum sensor (LI-COR model: LI192SA) were then used to convert the continuous monitoring light intensity data to photosynthetically active radiation (PAR). Water samples were taken weekly for measurements of inorganic nutrients ( $\text{NH}_4^+$ ,  $\text{NO}_x$ ,  $\text{PO}_4^{3-}$ ), chlorophyll a (Chl *a*), particulate organic carbon (POC), and DOC ( $n \text{ week}^{-1} = 4\text{--}6$ ).

## Benthic cover estimation

The reef community composition (% cover) at the study site was measured at the beginning of each seasonal period by line-point intercept (LPI) transects (Nadon and Stirling 2006), six 50 m transects, point interval 0.5 m,  $n = 600$  points per survey. Additionally, exposed reef sponge benthic cover was determined using 0.25 m<sup>2</sup> planar quadrats, ( $n = 15$  per survey) to better quantify small specimens in cracks. The ratio of benthic cover of cryptic sponges per projected reef area was set at 0.82 (i.e., m<sup>2</sup> sponge cover m<sup>-2</sup> planar reef surface), based on values obtained from an extensive survey on cryptic sponges from 25 cryptic habitats at the same study area (Richter et al. 2001). A set of 2D–3D conversion factors were used to convert the planar reef benthic cover data from the LPI transects to 3D surface areas (see online resource). The exposed reef sponge and cryptic sponge benthic cover data were already measured in 3D so did not require conversion.

## Benthic reef organism sampling and maintenance

Specimens of hard and soft corals, macroalgae, turf algae, coral rock, and sediment, as well as exposed reef and cryptic sponges, were collected from the reef for quantification of carbon fluxes. Eight specimens of four genera of hard corals (branching: *Acropora*, *Stylophora*, *Pocillopora*, massive: *Goniastrea*), one family and one genus

of soft corals (*Xeniidae*, and *Sarcophyton*), two genera of macroalgae (*Lobophora* and *Caulerpa*), as well as turf algal, sediment, and coral rock communities (each with epibiont communities that were not further differentiated) were collected from the study site. For the spring season, five individuals per sponge species—*Mycale fistulifera* (exposed reef), *Callyspongia* sp. and *Hemimycale arabica* (exposed reef and cryptic), and *Chondrilla sacchiformis* (cryptic)—were collected. These sponge species were found to be abundant on the investigated reef's surface or cavities (Wunsch et al. 2000; Kötter 2002). All specimens were maintained in an outside running seawater flow-through aquarium (800 L, flow-through 4000 L h<sup>-1</sup>) with water pumped directly from the reef at 10 m water depth and light conditions adjusted to in situ conditions at 10 m water depth using layers of plastic mesh.

## Metabolic rate measurements of benthic reef organisms and plankton

Closed cell respirometric incubations were conducted in the aquarium system described above to measure net photosynthesis ( $P_n$ ) at midday and dark respiration ( $R$ ) at night of plankton in the water column and all benthic functional groups as described in Tilstra et al. (2018) for plankton, Rix et al. (2017) for sponges, and van Hoytema et al. (2016) for other benthic groups. Measurements were standardized to specimen surface area using advanced geometry (Naumann et al. 2009). Photosynthetic and respiratory quotients were assumed to be 1 for all incubations (Gattuso et al. 1996; Carpenter and Williams 2007), leading to a direct conversion to measurements in mmol C L<sup>-1</sup> h<sup>-1</sup> for plankton and mmol C cm<sup>-2</sup> h<sup>-1</sup> for benthic functional groups. Plankton  $P_n$  and  $R$  were integrated over 10 m water column above the reef (i.e., 10 m<sup>3</sup> m<sup>-2</sup> planar reef surface). Gross primary production rates (GPP) were calculated as the sum of  $P_n$  and  $R$ , corrected for daylight hours and assuming equal nighttime and daytime respiration rates. Midday  $P_n$  rates were corrected for the difference in  $P_n$  over the entire day using a set of whole day  $P_n$  incubations covering various groups.  $R$  was multiplied by 24 h to obtain daily rates.

Organic matter uptake and release rates by hard and soft corals, macroalgae, turf algae, coral rock, and sponges were measured under the same conditions as described above, using the methods of Rix et al. (2017) for sponges and Naumann et al. (2010) for others. Measurements of DOC and POC concentrations at the start and end of the incubations were used to calculate DOC and POC uptake and release rates in mmol C cm<sup>-2</sup> specimen surface area h<sup>-1</sup>. See online resource for the extrapolation to daily rates.

## Linear inverse food web model (food web LIM)

A linear inverse model (LIM) was developed for each of the four seasons as well as an additional spring version, which includes the sponge community. A LIM consists of matrix equations with equalities and inequalities (Soetaert and van Oevelen 2009). The type of LIM used here assumes steady state for all compartments. Carbon fluxes into and out of each compartment, as well as the model as a whole, are balanced. Therefore, the model does not allow for net in- or decreases in biomass. However, coral reefs generally have a balanced production/respiration ratio, indicating minimal net growth (Hatcher 1988) and rates of net changes in biomass of reef communities are considered small compared to the magnitude of carbon fluxes between reef communities. Additionally, Vézina and Pahlow (2003) investigated the effect of the steady-state assumption in LIMs on simulated food webs which were in steady and transient state. They found that the steady-state assumption did not significantly alter the accuracy of the ecosystem flux reconstructions. Model constructions and solutions were run in R (version 3.0.2, R Development Core Team, 2013) using the R-package LIM (<http://lib.stat.cmu.edu/R/CRAN/web/packages/LIM/index.html>). The LIM food web topology is identical for all four seasons and consists of the water column and the coral reef benthos. The additional spring model adds the sponge community (both on the exposed outer reef and cryptic in cavities) to this model. The LIM in each season consists of 12 compartments and 60 fluxes while the spring sponges included model has 14 compartments and 75 fluxes (Fig. 1 and 2).

*The pelagic food web* — The pelagic food web consists of particulate organic carbon (POC), dissolved organic carbon (DOC), phytoplankton, and bacterioplankton. Both biotic compartments respire. In addition to this, phytoplankton perform photosynthesis and releases POC and DOC to the water column. Bacterioplankton feed on DOC and release DOC and POC. Finally, POC dissolves into DOC. As the fringing reef is hydrodynamically relatively open—the water residence time is measured in  $\text{h}^{-1}$ , compared to  $\text{yr}^{-1}$  for a Pacific atoll lagoon (Niquil et al. 1998; Naumann et al. 2012)—influxes of C (i.e., import of C from outside the reef ecosystem) are allowed for all water column compartments. The relative composition of this imported C (concentrations of DOC, POC, phytoplankton, and bacterioplankton) has to reflect the relative amounts of C for the water column compartments as calculated from the environmental monitoring and from literature on the study area (see online resource). The total amount of imported C was not defined in the model input. The model calculated this as the C needed in addition to GPP to meet R demand.

*The benthic food web* — The coral reef benthos consist of hard corals, soft corals, macroalgae, turf algae, coral

rock, sediment, and (for spring) exposed reef and cryptic sponges. All these compartments respire and photosynthesize, except for the cryptic sponges that only respire. Light levels for cryptic sponges were assumed too low for GPP. Hard and soft corals feed on bacterioplankton. Coral rock with its suspension- and filter-feeding communities does the same, but also feeds on phytoplankton (Yahel et al. 2006). In addition, all these compartments together with macroalgae and turf algae can take up and release POC and DOC. Hard and soft corals release mucus as POC into the water column, of which 56–80% dissolves into DOC (Wild et al. 2004). Additionally, there is a direct flux from hard corals to sediment based on the release of mucus strings (34–63% of hard coral POC release), which settle quickly to the sediment (Mayer and Wild 2010; Naumann et al. 2012). Both exposed reef and cryptic sponge compartments take up phytoplankton, bacterioplankton, POC and DOC, and release POC and DOC. Sediment biota and organic C pools were combined into a sediment organic carbon compartment, which photosynthesizes and respire and takes up and releases DOC while only taking up POC.

Export fluxes out of the reef system were created for macroalgae and turf algae to be able to balance the in- and effluxes for their compartments in certain seasons. An additional export flux was created for sediment to reduce a feedback loop from water column POC and DOC to sediment and back, which inflated those fluxes. Export for macroalgae was set to 3.7, 2.4, 8.8, and 0.0  $\text{mmol C m}^{-2} \text{d}^{-1}$  for winter, spring, summer, and fall, respectively. For turf algae, export was set to 0.0, 1.3, 0.8, and 0.0  $\text{mmol C m}^{-2} \text{d}^{-1}$ . For sediment, the export fluxes are 1.0, 1.2, 1.2, and 1.0  $\text{mmol C m}^{-2} \text{d}^{-1}$ . All these fluxes were set at their minimum level, and no other export fluxes were entered to ensure that estimates of C cycling remained conservative.

All data introduced to the model had been converted to  $\text{mmol C m}^{-2} \text{planar reef surface d}^{-1}$  and were added as ranges (inequalities) based on mean flux  $\pm 95\%$  confidence intervals (95-CI) to incorporate natural variability obtained from the respiratory measurements, or uncertainty of literature values. The only exception to this were the export fluxes from turf algae, macroalgae, and sediment as described above, which were entered as single values (equalities).

The models were solved for the flux values by a Monte-Carlo sampling method (Soetaert and van Oevelen 2009). Briefly, 10,000 food web structures were sequentially sampled resulting in 10,000 estimates for each C flux. All estimates were different, but consistent with the matrix equations constructed from the topology and entered values and ranges. The mean and standard deviation of the sample collection for each modeled flux as presented in the results section represent the best estimate and a measure of its uncertainty, respectively. The script files which contain the input

Ecosystem

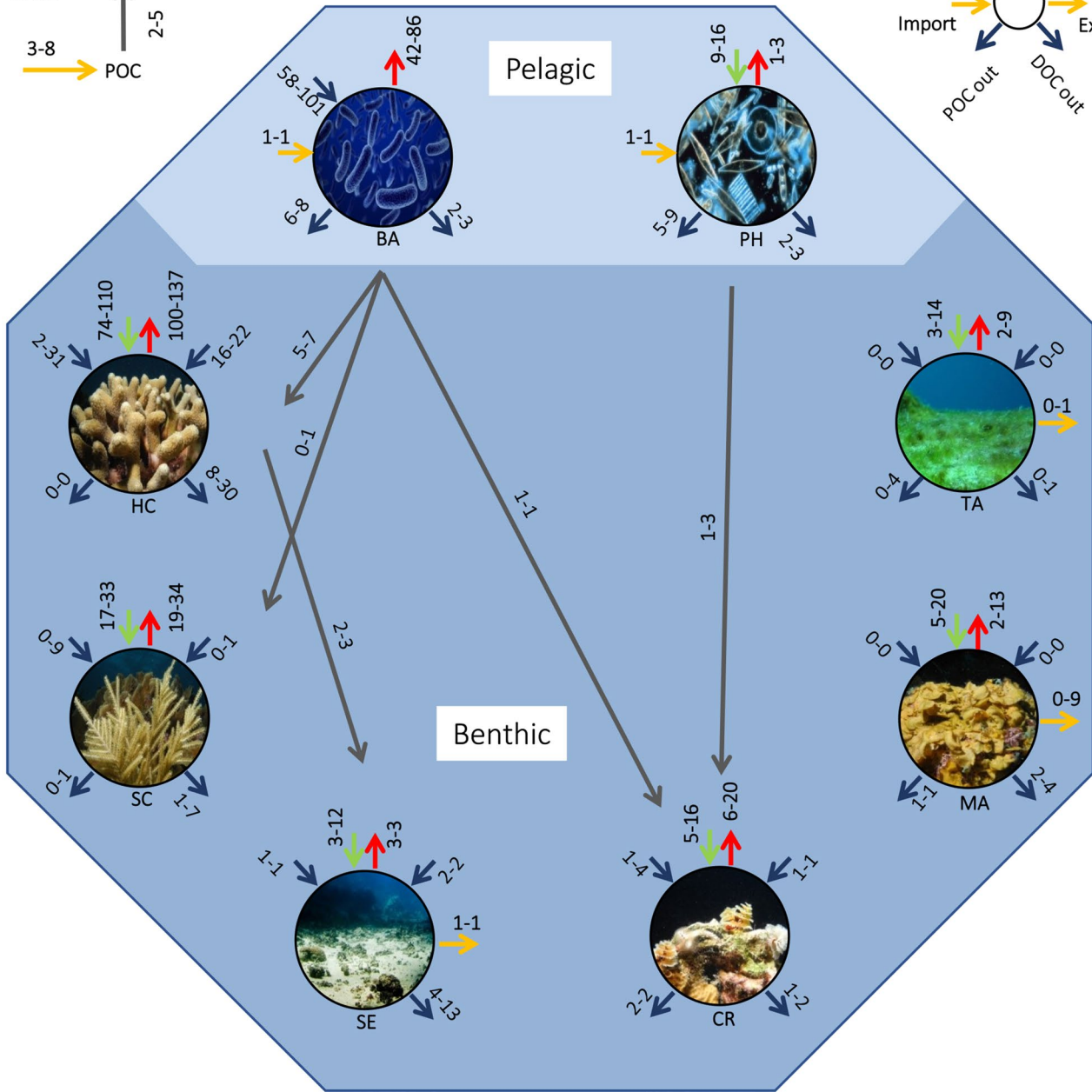
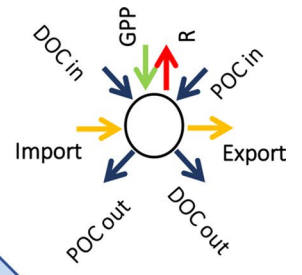
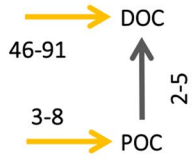


**Fig. 1** Ranges of seasonal means for all fluxes produced by the seasonal food web models in  $\text{mmol C m}^{-2} \text{planar reef d}^{-1}$ . Pelagic: BA = bacterioplankton, PH = phytoplankton; Benthic: TA = turf algae, MA = macroalgae, CR = coral rock, SE = sediment, SC = soft corals, HC = hard coralst. Fluxes around each functional group defined

by legend in top right corner. Gray arrows: fluxes between functional groups. Influxes of dissolved organic carbon (DOC) and particulate organic carbon (POC) and dissolution of POC to DOC given in top left corner

data and structure of the models are available at DOI: <https://doi.org/10.5281/zenodo.7534570>.

**Results**

In the results below, data will first be presented for the annual C-cycle model excluding the sponge community

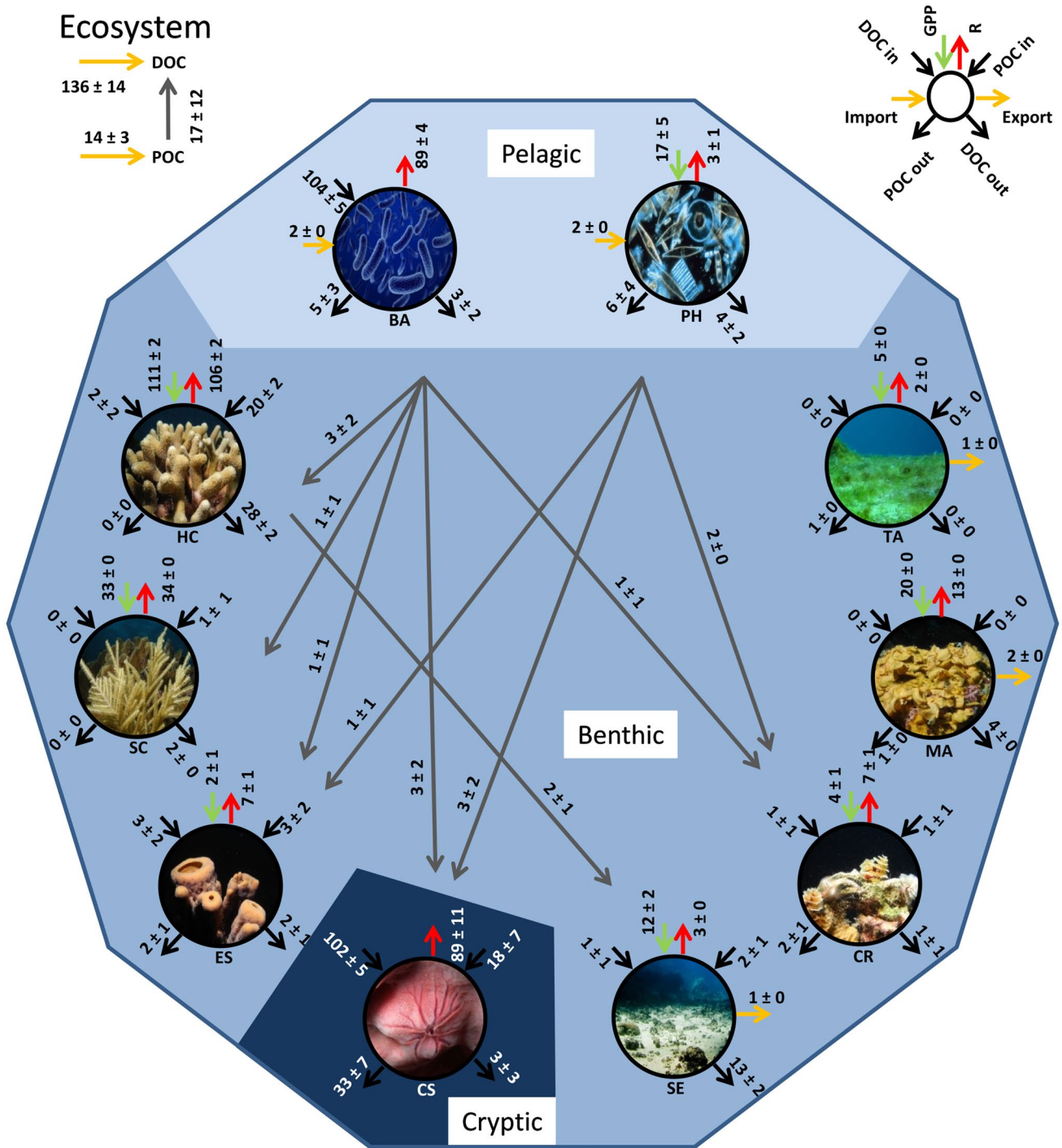


**Fig. 2** Mean  $\pm$  standard deviation for all fluxes produced by the spring inc. sponges food web model in  $\text{mmol C m}^{-2} \text{ planar reef d}^{-1}$ . Pelagic: BA=bacterioplankton, PH=phytoplankton; Benthic: TA=turf algae, MA=macroalgae, CR=coral rock, SE=sediment, ES=exposed reef sponges, SC=soft corals, HC=hard corals; Cryptic: CS=cryptic sponges. Fluxes around each functional group

defined by legend in top right corner. Gray arrows: fluxes between functional groups. Influxes of dissolved organic carbon (DOC) and particulate organic carbon (POC) and dissolution of POC to DOC given in top left corner. Fluxes into and out of each compartment may appear to not be balanced. This is due to rounding to the nearest integer

**Table 1** Seasonal measurements of environmental parameters in the research area at 10 m water depth

	Winter (Feb)	Spring (Apr)	Summer (Sep)	Fall (Nov)
Temperature (°C)	22.3 ± 0.1	22.4 ± 0.1	27.0 ± 0.2	24.9 ± 0.1
PAR (mol photons m <sup>-2</sup> d <sup>-1</sup> )	3.45 ± 0.26	5.76 ± 0.13	6.99 ± 0.32	3.80 ± 0.34
Ammonium (μmol L <sup>-1</sup> )	0.32 ± 0.09	0.46 ± 0.07	0.11 ± 0.01	0.28 ± 0.12
Phosphate (μmol L <sup>-1</sup> )	0.11 ± 0.01	0.10 ± 0.02	0.04 ± 0.02	0.04 ± 0.01
Nitrogen oxides (μmol L <sup>-1</sup> )	0.71 ± 0.15	0.56 ± 0.12	0.06 ± 0.02	0.22 ± 0.23
Chl <i>a</i> (μg L <sup>-1</sup> )	0.21 ± 0.03	0.21 ± 0.01	0.10 ± 0.01	0.19 ± 0.05
POC (μmol L <sup>-1</sup> )	6.16 ± 1.29	10.3 ± 3.0	7.96 ± 2.46	8.81 ± 0.98
DOC (μmol L <sup>-1</sup> )	72.9 ± 5.2	72.0 ± 7.5	90.5 ± 1.0	86.2 ± 2.5

Values are given as mean ± SD. Feb=February, Apr=April, Sep=September, Nov=November. PAR=photosynthetically active radiation. Nitrogen oxides = nitrate + nitrite concentrations. Chl *a* = chlorophyll *a*, POC=particulate organic carbon, DOC=dissolved organic carbon

followed by the additional spring model including the sponge community.

### Environmental and benthic cover monitoring

The environmental monitoring confirmed the expected seasonal variations in light, temperature, and inorganic nutrient concentrations within the ecosystem (Table 1).

The total reef surface area was dominated by hard corals (49%; Table 2) and soft corals (25%). Only 10% of the reef surface was covered by macro- and turf algae, which exhibited the largest relative seasonal changes in benthic cover. When including the sponges in spring, cryptic sponges comprised 18% of reef surface, joining hard (38%) and soft corals (21%) as groups with highest benthic cover. The exposed reef sponges covered the least of the reef surface at just 1.2%.

**Table 2** Annual average surface areas (in m<sup>2</sup> m<sup>-2</sup><sub>planar reef</sub>; see Online Resource table S4 for 3D/2D conversion factors used), seasonal standard deviation (SD) and seasonal coefficient of variance (CV) are given of dominant benthic functional groups and substrates in the study area. Exposed reef and cryptic sponge surface areas are only

	Surface area (m <sup>2</sup> m <sup>-2</sup> <sub>planar reef</sub> )			Seasonal difference (% from annual mean)			
	Average	SD	CV	Winter	Spring	Summer	Fall
Hard corals	1.74	0.08	5				
Soft corals	0.88	0.09	11				
Macroalgae	0.22	0.08	37	-21	43	17	-39
Turf algae	0.15	0.14	96	142	-30	-71	-41
Bare substrate	0.34	0.05	14				
Sediment	0.25	0.03	13				
Seasonal surface total	3.58						
Exposed reef sponges Spring	0.05	N/A	N/A				
Cryptic sponges Spring	0.82*	N/A	N/A				

N/A = not applicable; \*Cryptic sponges were taken from Richter et al. (2001)

### Model-resolved carbon fluxes

To compare model results for different compartments in a concise way, values will be presented below as “annual mean ± SD, range over seasons”. When specific seasons are compared, values will be presented as seasonal mean ± SD. The mean values of fluxes (all in mmol C m<sup>-2</sup><sub>planar reef</sub> d<sup>-1</sup> throughout text unless stated otherwise) returned by the four seasonal models and the sponge model fell within five orders of magnitude (10<sup>-2</sup>–10<sup>2</sup>), except for certain fluxes in winter, summer, and fall for macroalgae and turf algae (DOC and POC uptake), which the model put at 0 to balance fluxes in and out of their compartments (Fig. S1–S5).

The largest annual mean influx of C into the ecosystem was the gross primary production (GPP) rate of hard corals (93 ± 16, 74–110; Fig. 1), followed by the import of DOC to the reef (67 ± 23, 46–91), which exceeded hard coral GPP in fall (82 ± 4 and 84 ± 10 for fall hard coral GPP and DOC

for spring. Benthic cover (%) per functional group is given based on the total surface area. For functional groups with a seasonal CV > 15, differences from the mean annual surface area (%) are given for each season.

import, respectively). Further major influxes of C were GPP for soft corals ( $24 \pm 6$ , 17–33), phytoplankton ( $14 \pm 5$ , 9–16), macroalgae ( $13 \pm 6$ , 5–20), and coral rock ( $10 \pm 4$ , 5–16). The largest C effluxes from the ecosystem were represented by respiration (R) rates of hard corals ( $112 \pm 17$ ; 100–137; the annual mean largest flux in the model), bacterioplankton ( $70 \pm 18$ ; 42–86), soft corals ( $26 \pm 6$ ; 19–34), and coral rock ( $12 \pm 5$ ; 6–20) (Fig. 1).

The C influxes *within* the ecosystem were dominated by the uptake of DOC by bacterioplankton ( $86 \pm 18$ ; 58–101; third largest flux derived from the model), followed by hard corals POC uptake ( $19 \pm 5$ ; 16–22) and DOC uptake ( $16 \pm 13$ ; 2–31) (Fig. 1). Largest release rates of C *within* the ecosystem were DOC release by hard corals ( $18 \pm 11$ ; 8–30) and the sediment community ( $8 \pm 4$ ; 4–13), followed by POC release by phytoplankton ( $8 \pm 4$ ; 5–9) and bacterioplankton ( $7 \pm 4$ ; 6–8) (Fig. 1).

The addition of sponges to the spring model required the import of DOC ( $136 \pm 14$ ) to overtake hard coral GPP ( $111 \pm 2$ ) as the largest influx of C to the ecosystem. Cryptic sponges R ( $89 \pm 11$ ) joined bacterioplankton R ( $89 \pm 4$ ) as the largest C effluxes next to hard coral R ( $106 \pm 2$ ) (Fig. 2). The dominant C fluxes *within* the ecosystem in the sponge-added spring model were cryptic sponges DOC uptake ( $102 \pm 5$ ) and bacterioplankton DOC uptake ( $104 \pm 5$ ), followed by cryptic sponge POC release ( $33 \pm 7$ ).

### Ecosystem productivity and seasonal C-budgets

Total GPP was highest in spring and summer ( $200 \pm 7$  and  $190 \pm 7$ , respectively; annual mean  $167 \pm 29$ ), while total R was highest in summer followed by spring ( $279 \pm 15$  and  $247 \pm 7$ , respectively; annual mean  $236 \pm 33$ ; Fig. 3). GPP and R reef ecosystem rates resulted in daily GPP:R ratios of  $0.75 \pm 0.05$  and  $0.81 \pm 0.04$  in winter and spring, respectively, which decreased into summer ( $0.68 \pm 0.04$ ) and fall ( $0.60 \pm 0.04$ ), indicating that the reef carbon balance was always net heterotrophic (i.e., GPP:R < 1), and most heterotrophic in summer and fall (Fig. 3).

Hard and soft corals were the dominant contributors to reef ecosystem GPP (Fig. 4). Their combined contribution ranged from 63% in winter to 77% in fall. Phytoplanktonic GPP was relatively stable and contributed between 6 (fall) and 11% (winter) to total GPP. The increase in hard coral GPP from  $74 \pm 5$  to  $110 \pm 2$  from winter to spring is primarily responsible for the highest total GPP rate in spring (Fig. 4). The main contributors to R were the hard corals (40–53%) and bacterioplankton (22–35%), Fig. 4). The increase in bacterioplankton R from  $42 \pm 3$  to  $86 \pm 7$  from winter to spring was the main driver behind the increase in total R from winter to spring, while hard coral R remained stable ( $101 \pm 9$  to  $100 \pm 5$ ). The subsequent increase in hard coral R to  $137 \pm 11$  in summer with bacterioplankton R

remaining stable (Fig. 4) caused summer to be the highest season for total R (Fig. 3).

Total influx of C (i.e., the sum of GPP and import of external organic C) increased strongly from  $197 \pm 10$  in winter to  $290 \pm 15$  in summer and then decreased again in fall ( $228 \pm 9$ ) (Table 3). Over the seasons, the relative importance of GPP and import of organic C to balance R changed as the system became more heterotrophic from spring into summer and fall. The ratio between total GPP and total external organic C import decreased from 2.9 and 4.1 in winter and spring to 2.0 and 1.5 in summer and fall, respectively (Fig. 3, Table 3). Seasonal organic C influx to, and uptake by, reef communities was dominated by DOC, constituting 88–92 and 79–85% of total organic C influx and uptake, respectively (Fig. 1, Table 3). POC played a much smaller role in the system's C cycle than DOC. Biotic uptake of POC (annual mean  $23 \pm 5$ ) was a fifth of the uptake of DOC (annual mean  $110 \pm 23$ ) and changed little over the seasons. In contrast, DOC uptake increased strongly from winter ( $78 \pm 10$ ) to summer and fall ( $122 \pm 14$  and  $131 \pm 13$ ), reaching the same order of magnitude as GPP and R rates (Table 3).

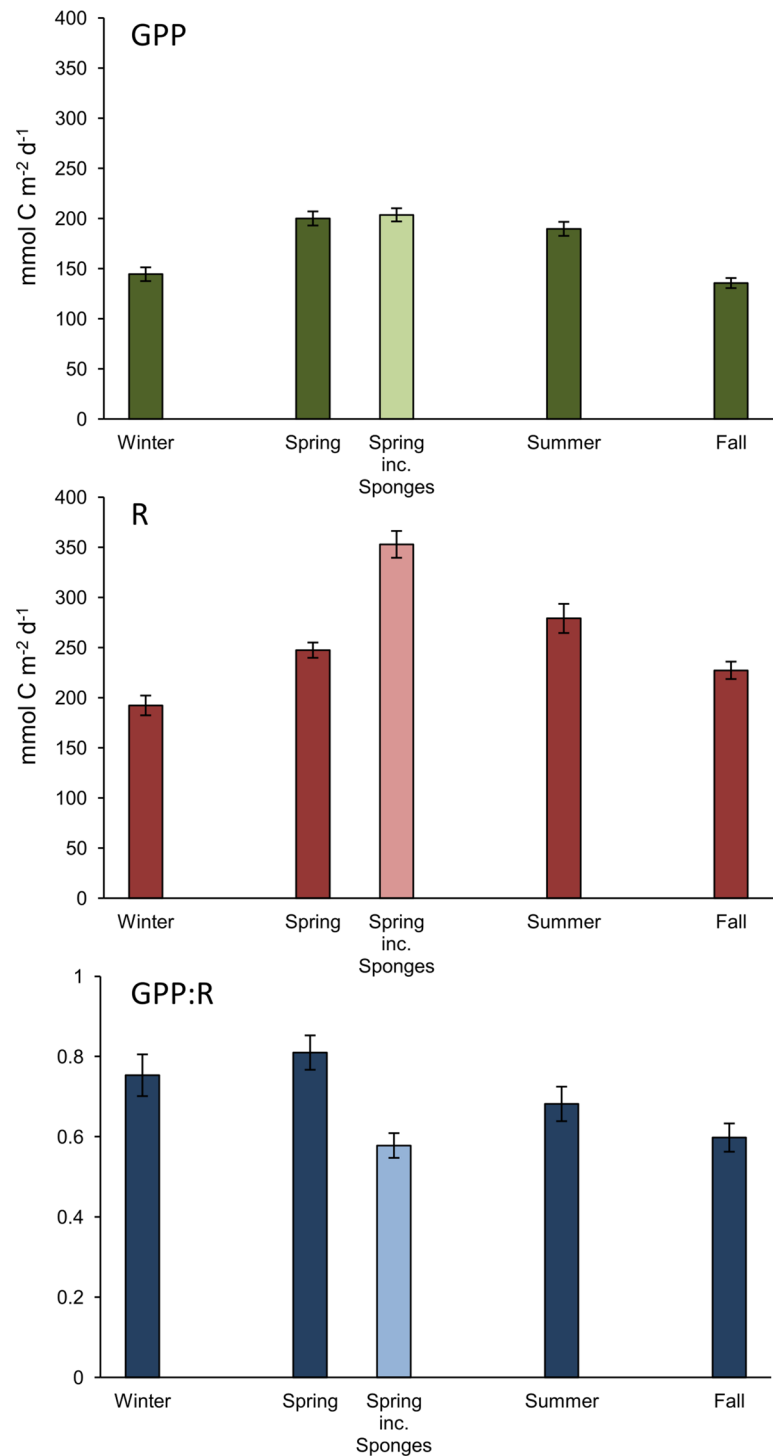
Grazing on phytoplankton ( $2 \pm 1$ ; 1–3) and bacterioplankton ( $8 \pm 4$ ; 7–9) by reef benthos showed no substantial seasonal differences and were among the smallest fluxes in the model. (Fig. 1, Table 3).

The addition of sponges to the spring model made the system more heterotrophic. While GPP increased little (from  $200 \pm 7$  to  $204 \pm 7$ ), R increased substantially from  $247 \pm 8$  to  $353 \pm 13$ . This caused GPP:R to decrease from  $0.81 \pm 0.04$  to  $0.58 \pm 0.03$  (Fig. 3). Cryptic sponges joined bacterioplankton and hard corals as the main drivers of system R contributing 25, 25 and 30% of the total R, respectively (Fig. 4). The relative importance of GPP and import of organic C to balance R changed drastically as the ratio between total GPP and total external C import decreased from 4.1 to 1.3 (Fig. 5). The addition of sponges did not alter the relative importance of DOC for organic C import or uptake. While DOC and POC uptake both more than doubled ( $105 \pm 8$  to  $214 \pm 9$  and  $20 \pm 3$  to  $47 \pm 8$ , respectively), their ratio remained similar at DOC uptake being five times POC uptake. While DOC release remained comparable ( $57 \pm 5$  to  $61 \pm 8$ ), adding the sponges strongly increased system POC release from  $17 \pm 3$  to  $50 \pm 9$ . While sponges do filter-feed on plankton, their addition caused only a minor increase in predation on phytoplankton and bacterioplankton ( $2 \pm 1$  to  $6 \pm 2$  and  $7 \pm 3$  to  $10 \pm 3$ , respectively).

Overall, the fluxes in the inverse models appear well constrained, especially so for the larger and therefore more important fluxes (Fig. S1–S5) as also evidenced by the coefficient of variation (CoV, i.e., standard deviation normalized to its corresponding mean). When we investigate the CoV for fluxes into and out of each compartment (Table 4), we



**Fig. 3** Seasonal reef community metabolism. Values are mean  $\pm$  SD. GPP=gross primary production, R=respiration, GPP:R=gross primary production to community respiration ratio



find that the mean CoV per compartment falls below 0.5 for most compartments in most seasons. Fluxes mediated by macroalgae and turf algae show very low CoV because their mass balance required them to be at their minimum or maximum levels for the model to be solvable. Breaking the CoVs down per type of flux (Table 4) shows that import, GPP, and R fluxes are more constrained while the internal DOC-, POC- and predation-related fluxes were less constrained.

## Discussion

This study is the first annual carbon (C) cycle model for a Red Sea coral reef ecosystem that specifically incorporates seasonal variation and sponges. The model shows that the northern Red Sea coral reef ecosystem is net heterotrophic (i.e., gross community primary production

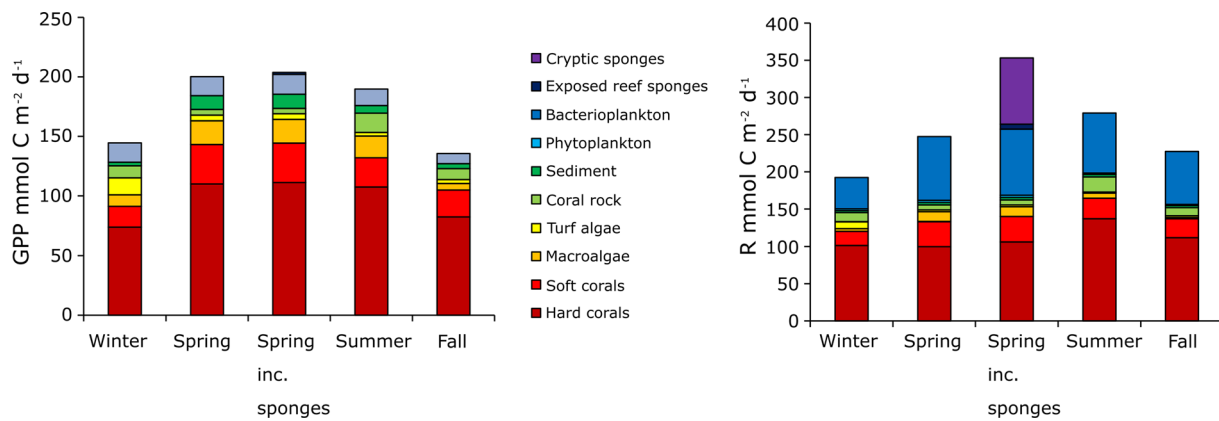


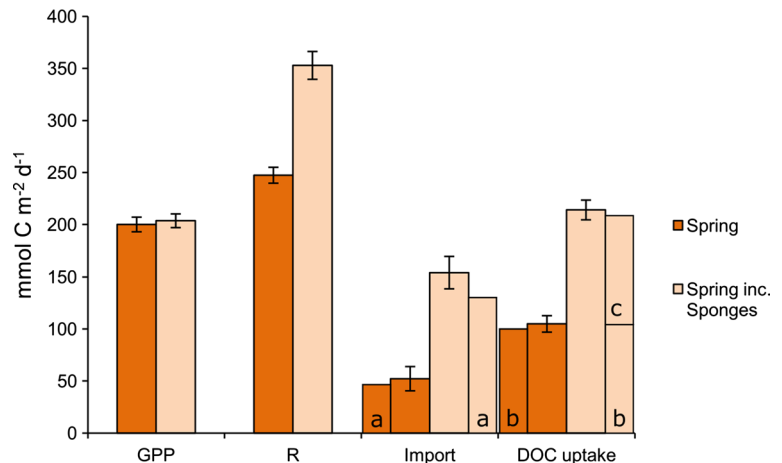
**Fig. 4** Seasonal mean gross primary production (GPP) and respiration (R) for various functional groups. The GPP graph does not contain data for bacterioplankton or cryptic sponges

**Table 3** Modeled seasonal carbon cycling by the system as a whole.

	Winter	Spring	Spring sponges	Summer	Fall
GPP	144 ± 7	200 ± 7	204 ± 7	190 ± 7	136 ± 5
Import	53 ± 12	52 ± 12	154 ± 16	100 ± 16	93 ± 11
R	192 ± 10	247 ± 8	353 ± 13	279 ± 15	227 ± 9
Export	5 ± 0	5 ± 0	5 ± 0	11 ± 0	1 ± 0
DOC uptake	78 ± 10	105 ± 8	214 ± 9	122 ± 14	131 ± 13
DOC release	24 ± 5	57 ± 5	61 ± 8	29 ± 5	44 ± 11
POC uptake	21 ± 4	20 ± 3	47 ± 8	27 ± 5	22 ± 4
POC release	23 ± 5	17 ± 3	50 ± 9	22 ± 5	17 ± 4
Predation	10 ± 4	9 ± 3	16 ± 4	10 ± 4	9 ± 4

Community gross primary production (GPP), organic carbon import, community respiration (R), organic carbon export, uptake and release of dissolved organic carbon (DOC) and particulate organic carbon (POC), and predation by all functional groups. Values in  $\text{mmol C m}^{-2} \text{ planar reef d}^{-1}$ , (mean ± SE). Predation is the sum of all fluxes between functional groups, except hard coral mucus deposition to sediment

**Fig. 5** Major system C fluxes in spring with and without sponges. GPP = gross primary production, R = respiration, Import = import of organic C into the system; a = dissolved organic carbon (DOC) as part of import, DOC uptake is biotic DOC uptake in the system; b = bacterioplankton as part of DOC uptake; c = sponges as part of DOC uptake



(GPP) < community respiration (R)) and balanced by C import, predominantly of dissolved organic carbon (DOC).

### Seasonal Red Sea C cycling: main ecosystem processes

The ranges—all rates in  $\text{mmol C m}^{-2} \text{ planar reef d}^{-1}$  throughout text, unless stated otherwise—of seasonal mean GPP (136–200), R (192–279) and GPP:R (0.6–0.8) ratios are comparable, but at the lower end of rates found for other coral reefs (Table 5). Ecosystem primary productivity was highest and comparable in spring and summer, coinciding with highest levels of irradiance. Respiration was higher than GPP in all seasons with highest respiration in spring and summer, although the GPP:R ratios were lowest in summer and fall, the seasons with highest water temperature. Looking at the seasonal response of the reef, a community metabolism study for a nearby Israeli reef crest (Silverman et al. 2007) found a similar trend. For both the Israeli reef and our Jordanian reef, GPP and R were higher during

**Table 4** Coefficients of variation (standard deviation/corresponding mean) for the model fluxes averaged per (a) compartment they flow into/out of, and (b) type of flux

a.	Winter	Spring	Spring inc. Sponges	Summer	Fall
Phytoplankton	0.34	0.32	0.45	0.30	0.37
Bacterioplankton	0.50	0.46	0.52	0.50	0.48
POC	0.42	0.38	0.41	0.42	0.41
DOC	0.46	0.41	0.42	0.46	0.41
Hard corals	0.35	0.27	0.27	0.34	0.29
Hco_POC	0.43	0.28	0.42	0.43	0.39
Soft corals	0.43	0.33	0.32	0.45	0.40
Sco_POC	0.33	0.20	0.20	0.31	0.34
Macroalgae	0.00	0.24	0.25	0.00	0.30
Turf algae	0.00	0.25	0.25	0.00	0.31
Coral rock	0.43	0.44	0.44	0.46	0.43
Sediment	0.28	0.23	0.26	0.23	0.22
Exposed reef sponges			0.57		
Cryptic sponges			0.47		
b.	Winter	Spring	Spring inc. Sponges	Summer	Fall
Import	0.24	0.25	0.14	0.21	0.20
GPP	0.12	0.11	0.17	0.09	0.10
Respiration	0.11	0.09	0.09	0.12	0.11
Internal DOC fluxes	0.47	0.47	0.47	0.48	0.48
Internal POC fluxes	0.44	0.46	0.47	0.43	0.50
Internal predation fluxes	0.56	0.50	0.65	0.57	0.56

Color coding from blue = low to red = high

**Table 5** Comparison of metabolic parameters with literature

Site	GPP	R	GPP:R	Reference
Aqaba, Jordan, reef slope, seasonal range	<b>136–200</b>	<b>192–279</b>	<b>0.6–0.8</b>	<b>This study</b>
Aqaba, Jordan, reef slope, spring inc. sponges	<b>204</b>	<b>353</b>	<b>0.6</b>	<b>This study</b>
Aqaba, Jordan, reef slope, annual average	268	154	1.7	Cardini et al. (2016)
Eilat, Israel, reef crest, winter	260	180	1.4	Silverman et al. (2007)
Eilat, Israel, reef crest, summer	400	390	1.0	Silverman et al. (2007)
French Frigate Shoals, reef flat, winter	356	213	1.7	Atkinson and Grigg (1984)
French Frigate Shoals, reef flat, summer	710	405	1.8	Atkinson and Grigg (1984)
Kaneohe Bay, Hawaii, USA, reef flat	400	465	0.9	Lowe and Falter (2015)
Florida Keys, USA, reef crest	944	566	1.7	Long et al. (2013)
Florida Keys, reef slope	193	199	0.97	Long et al. (2013)
Colombian Caribbean, reef slope, seasonal range	250–305	136–146	1.7–2.2	Eidens et al. (2014)
Various Caribbean/Pacific, reef slope	167–583	158–250	0.5–5.5	Hatcher (1988)

All values in  $\text{mmol C m}^{-2} \text{d}^{-1}$  given as means or ranges. GPP = gross primary production, R = community respiration, GPP:R = gross primary production to community respiration ratio. An  $\text{O}_2$ :C ratio of 1 was assumed when transforming  $\text{O}_2$  to C fluxes (Gattuso et al. 1996; Carpenter and Williams 2007)

summer when both light availability and water temperature were high, than in winter when these parameters were lower.

Taking the average across seasons, hard corals contributed most to system GPP (56%) and R (48%). In the seasonal model without sponges, bacterioplankton DOC uptake was the largest internal flux at  $86 \pm 18$ . This estimate of the microbial loop over a coral reef is slightly above previous

estimates (5–50, de Goeij et al. 2013). The reef system relies on external organic C (particularly DOC) to offset the difference between R and GPP. Direct comparisons between GPP and import of organic C to reefs in literature are rare, but the relative importance of import here (annual mean 46% of GPP) is larger than a previous estimate (15% of GPP) for a Pacific reef flat. However, that estimate did not include DOC

fluxes (Alldredge et al. 2013), which are the largest C fluxes contributing to import here.

The import of C into a coral reef from offshore happens through convective transport across a turbulent boundary layer. This turbulence is enhanced by the reef's rugosity (Lowe and Falter 2015). Drag coefficients for an Israeli reef close to the reef studied here were found to be 3 to 5 times higher than a nearby sandy site (Reidenbach et al. 2006). In many reefs, an additional factor enhancing mass transfer to the reef is wave-driven oscillatory flows increasing water flow within the reef, thereby enhancing exchange (Lowe and Falter 2015). However, the reefs of the northern Gulf of Aqaba experience relatively little wave action (Reidenbach et al. 2006). Another study on diurnal water movement around a nearby Israeli reef found a cycle where surface water temperature changes across the day drove currents that moved water into the reef from offshore (Genin et al. 2002). Such a cycle might well exist in the reef studied here, continually importing new organic C to meet the reef's metabolic demand.

### The addition of the sponge community to a Red Sea coral reef C budget

The addition of the sponge community to the spring model causes major changes to the ecosystem. These changes were mainly driven by the cryptic sponge community in our study site, since cryptic sponges were on average 16 times more abundant than the exposed reef sponges. Rates of sponge community DOC uptake and R are comparable to bacterioplankton, which substantially increases the heterotrophy of the ecosystem.

The cryptic habitat on coral reefs is often overlooked, since most coral reef benthic surveys use traditional 2D photographs (de Goeij et al. 2017; Kornder et al. 2021). This causes a remarkable oversight, given that the cryptic habitat can represent more than half of the total volume, surface, and benthic biomass of the reef (Ginsburg 1983; Richter et al. 2001; Kornder et al. 2021). In our study area, the cryptic reef surface was found to be up to 7.5 m<sup>2</sup> per projected m<sup>2</sup> reef surface (Richter et al. 2001).

Our model estimates are in line with evidence that the cryptic habitat is a major sink of DOC (de Goeij and van Duyl 2007) and that many sponges drive ecosystem productivity by shunting DOC to higher trophic levels as POC (de Goeij et al. 2013, 2017; Rix et al. 2016, 2018). First (rough) estimations of DOC cycling through the sponge loop (90–350) were in the same order of magnitude as community GPP (200–600) and higher than the well-established microbial loop on a Caribbean reef (5–50) (de Goeij et al. 2013). Indeed, at the Aqaba reef system, the sponge loop DOC uptake ( $105 \pm 6$ ) is in the same order of magnitude as GPP ( $199 \pm 7$ ), while the microbial loop DOC uptake rates

( $104 \pm 5$ ) are comparable to the sponge loop in terms of carbon cycling.

Release rates of POC by sponges are estimated as an important flux ( $35 \pm 7$ ), representing a large potential food source for higher trophic levels, such as detritivores. Most sponges tested in the mentioned literature have an encrusting growth form, i.e., following the contours of the reef surface. Recent studies have shown that massive, upward-growing sponges that are often dominant on the exposed reef surface, including in the Red Sea (but not in our study area), show a fundamentally different C cycling than encrusting sponges. Several massive sponge species did not produce significant amounts of POC after DOC uptake (McMurray et al. 2018; Wooster et al. 2019), and some species with low abundances of associated microbes showed limited DOC uptake or a net release (Hoer et al. 2018; Olinger et al. 2021). This led to a sponge loop hypothesis based on spongivory, rather than C cycling through POC (Pawlik and McMurray 2020). Recently, both hypotheses were tested valid for two deep-sea sponge species, although no clear evidence pointed to either one (Bart et al. 2021). Moreover, in another recent study it was shown that (massive) sponges can "sneeze" and release detritus from their inflow (not outflow) openings and may have caused this detritus production undetected in earlier studies (Kornder et al. 2022). Our study supports that cryptic sponges act as ecological engines (de Goeij et al. 2017) and have the potential to drive carbon and nutrient cycling on coral reefs (Maldonado et al. 2012).

These results indicate that reefs including their cryptic sponge community may behave far more heterotrophic than previous reef metabolism studies indicated and that certain reef ecosystems may be more reliant on external sources of nutrients (Atkinson 2011). Indeed, as oceans warm, corals are expected to become more heterotrophic due to increased respiration (Bahr et al. 2018), as was found here with substantially lower GPP:R in warmer summer than in spring even though light availability increased as well.

### Limitations and future considerations

The models presented here are based on extensive field data of C fluxes directly measured on the functional groups of the Aqaba reef. However, any ecosystem-based model comes with uncertainties and assumptions. For example, we assumed stable respiration rates over a 24-h cycle. However, respiration rates are most likely underestimated due to higher R rates under higher light regimes (e.g., Kuhl et al. 1995; Schrammeyer et al. 2014), negatively affecting P<sub>n</sub> and thus GPP, since R measurements were all done at night. Increased respiration in the light remains an important, but illusive parameter in coral reef metabolism research. It should also be noted that the extensive dataset of C fluxes was collected through aquarium incubations. The water used

was directly pumped from the reef area at 10 m depth, light was adjusted based on in situ measurements, and incubation duration was limited to prevent effects like hyperoxia due to photosynthesis, but incubations of specimens outside of their environment will always introduce incubation effects. Water movement included in the incubations will never be fully comparable to the complex water movement across a full coral reef in situ (Shashar et al. 1996). Additionally, the biochemical composition of coral reef water can vary across the reef (van Duyl and Gast 2001) and be particularly distinct inside cavities (de Goeij and van Duyl 2007). However, except uncertainties predicting precise ecosystem GPP,  $R$ , and  $P_n$ , overall reef C fluxes from our LIM show representative dominant seasonal trends and patterns within the C food web.

Additionally, the walls of coral reef cavities are almost 100% covered with “coelobites”, mostly filter-feeding organisms—e.g., tunicates, bryozoans, polychaetes, dominated by sponges—but also include communities of primary producers, such as crustose coralline algae, soft- and hard corals (Jackson and Winston 1982; van Duyl et al. 2006; Kornder et al. 2021; Vicente et al. 2021). This study did not include the non-sponge heterotrophic and autotrophic cryptic communities due to a lack of data, and therefore, their impact on C cycling remains unknown.

We also used surface cover as metric to calculate rates on exposed reef and cryptic habitat. From a biogeochemical perspective, it would be better to use the metric biomass, such as (ash-free) dry weight or organic carbon, to determine food web rates (de Goeij et al. 2017; Kornder et al. 2021). The 2D–3D conversion to projected cover presented in this study is already an enormous improvement, but still discards different surface-to-volume ratios of organisms, underestimating erect organism (e.g., soft corals, massive sponges) compared to non-erect organisms (e.g., non-branching corals, algae, encrusting sponges). Kornder et al. (2021) tested these metric conversions in Curaçao and found that traditional 2D surface cover surveys (excluding the cryptic habitats) estimated non-calcifying phototrophs and scleractinian corals to be the largest benthic groups. However, the 3D biomass (ash-free dry weight) survey, including the cryptic habitats, estimated sponges to be the largest group. In fact, half of the available surface and of the benthic biomass was estimated to be residing in the cryptic habitats of the reef.

## Conclusions

Here, we provided a first reef-wide estimation of carbon cycling throughout four seasons in the Red Sea and a first quantification of the role that sponges play in such a reef.

The model shows that previously understudied and neglected functional groups and carbon pools can be major players in coral reef carbon cycling. It is vital for future coral reef research and conservation to include organisms, nutrients, and processes we cannot see, but which are important: the role of organisms in the cryptic habitat as well as the role of micro- and microbial processing of dissolved organic matter. Processes of recent reef decline are well described and global effects are well studied, and we are beginning to understand the ecological processes underlying these changes (Rädecker et al. 2014; Santos et al. 2014; Roth et al. 2021). However, it is very likely that the less visible functional groups and processes will play a large role in how reef functioning will change. The findings presented here highlight the need for key ecosystems drivers such as DOM, microbes, and sponges, to be incorporated into future ecological studies and conservation management strategies.

**Acknowledgements** We would like to thank S. Basyoni and S. Helber for assistance in the field, as well as C. Staschok, M. Birkicht, and D. Dasbach for field work preparation and sample analyses, and R. M. van der Ven for proofreading the manuscript.

**Author contributions** Conceptualization was performed by NvH, JMdG, DvO, LR, MSN, CW; method design by NvH, YEK, LR, MSN, CW; fieldwork by NvH, LR, UC, VNB, MSN; model development by NvH, JMdG, NAK, DvO; funding acquisition by CW; supervision by JMdG, DvO, MSN, CW; resources by FAH, CW; writing—original draft preparation—by NvH; writing—review and editing—by all authors.

**Funding** This study was funded by German Research Foundation Grant Wi 2677/6-1 to CW and the European Research Council (ERC starting Grant agreement #715513 to JMdG). VNB was funded by a stipend of “Evangelisches Studienwerk Villigst e.V.”.

## Declarations

**Conflict of interest** All authors certify that they have no affiliations with or involvement in any organization or entity with any financial interest or non-financial interest in the subject matter or materials discussed in this manuscript.

**Open Access** This article is licensed under a Creative Commons Attribution 4.0 International License, which permits use, sharing, adaptation, distribution and reproduction in any medium or format, as long as you give appropriate credit to the original author(s) and the source, provide a link to the Creative Commons licence, and indicate if changes were made. The images or other third party material in this article are included in the article’s Creative Commons licence, unless indicated otherwise in a credit line to the material. If material is not included in the article’s Creative Commons licence and your intended use is not permitted by statutory regulation or exceeds the permitted use, you will need to obtain permission directly from the copyright holder. To view a copy of this licence, visit <http://creativecommons.org/licenses/by/4.0/>.

## References

- Alexander BE, Liebrand K, Osinga R, van Der Geest HG, Admiraal W, Cleutjens JPM, Schutte B, Verheyen F, Ribes M, van Loon E, de Goeij JM (2014) Cell turnover and detritus production in marine sponges from tropical and temperate benthic ecosystems. *PLoS One* 9:e109486
- Allredge AL, Carlson CA, Carpenter RC (2013) Sources of organic carbon to coral reef flats. *Oceanography* 26:108–113
- Atkinson MJ (2011) Biogeochemistry of nutrients. In: Dubinsky Z, Stambler N (eds) *Coral reefs: an ecosystem in transition*. Springer Netherlands, Dordrecht, pp 199–206. [https://doi.org/10.1007/978-94-007-0114-4\\_13](https://doi.org/10.1007/978-94-007-0114-4_13)
- Atkinson MJ, Grigg RW (1984) Model of a coral reef ecosystem - II. Gross and net benthic primary production at French Frigate Shoals Hawaii. *Coral Reefs* 3:13–22
- Bahr KD, Rodgers KS, Jokiel PL (2018) Ocean warming drives decline in coral metabolism while acidification highlights species-specific responses. *Mar Biol Res* 14:924–935
- Bart MC, Hudspeth M, Rapp HT, Verdonschot PFM, de Goeij JM (2021) A deep-sea sponge loop? Sponges transfer dissolved and particulate organic carbon and nitrogen to associated fauna. *Front Mar Sci* 8:604879
- Berumen ML, Voolstra CR, Daffonchio D, Agusti, Aranda M, Irigoien X, Jones BH, Morán XAG, Duarte CM (2019) The Red Sea: environmental gradients shape a natural laboratory in a Nascent Ocean. In: Voolstra CR, Berumen ML (eds) *Coral Reefs of the Red Sea*. Springer International Publishing, Cham, pp 1–10. [https://doi.org/10.1007/978-3-030-05802-9\\_1](https://doi.org/10.1007/978-3-030-05802-9_1)
- Cardini U, Bednarz VN, van Hoytema N, Rovere A, Naumann MS, Al-Rshaidat MMD, Wild C (2016) Budget of Primary Production and Dinitrogen Fixation in a Highly Seasonal Red Sea Coral Reef. *Ecosystems* 19:771–785
- Carlson DF, Fredj E, Gildor H (2014) The annual cycle of vertical mixing and restratification in the Northern Gulf of Eilat/Aqaba (Red Sea) based on high temporal and vertical resolution observations. *Deep Res Part I Oceanogr Res Pap* 84:1–17
- Carpenter RC, Williams SL (2007) Mass transfer limitation of photosynthesis of coral reef algal turfs. *Mar Biol* 151:435–450
- Eidens C, Bayraktarov E, Hauffe T, Pizarro V, Wilke T, Wild C (2014) Benthic primary production in an upwelling-influenced coral reef, Colombian Caribbean. *PeerJ* 2014:e554
- Gattuso JP, Pichon M, Delesalle B, Canon C, Frankignoulle M (1996) Carbon fluxes in coral reefs. I. Lagrangian measurement of community metabolism and resulting air-sea CO<sub>2</sub> disequilibrium. *Mar Ecol Prog Ser* 145:109–121
- Genin A, Yahel G, Reidenbach MA, Monismith SG, Koseff JR (2002) Intense benthic grazing on phytoplankton in coral reefs revealed using the control volume approach. *Oceanography* 15:90–96
- Ginsburg RN (1983) Geological and biological roles of cavities in coral reefs. *Perspect Coral Reefs*.
- de Goeij JM, van Duyl FC (2007) Coral cavities are sinks of dissolved organic carbon (DOC). *Limnol Oceanogr* 52:2608–2617
- de Goeij JM, van den Berg H, van Oostveen MM, Epping EHG, van Duyl FC (2008) Major bulk dissolved organic carbon (DOC) removal by encrusting coral reef cavity sponges. *Mar Ecol Prog Ser* 357:139–151
- de Goeij JM, van Oevelen D, Vermeij MJA, Osinga R, Middelburg JJ, de Goeij AFPM, Admiraal W (2013) Surviving in a marine desert: The sponge loop retains resources within coral reefs. *Science* (80-) 342:108–110
- de Goeij JM, Lesser MP, Pawlik JR (2017) Nutrient fluxes and ecological functions of coral reef sponges in a changing ocean. In: Carballo, J., Bell, J. (eds) *Climate Change, Ocean Acidification and Sponges*. Springer, Cham. [https://doi.org/10.1007/978-3-319-59008-0\\_8](https://doi.org/10.1007/978-3-319-59008-0_8)
- Hatcher BG (1988) Coral reef primary productivity: a beggar's banquet. *Trends Ecol Evol* 3:106–111
- Heymans JJ, Coll M, Libralato S, Morissette L, Christensen V (2014) Global patterns in ecological indicators of marine food webs: A modelling approach. *PLoS One* 9:e95845
- Hoer DR, Gibson PJ, Tommerdahl JP, Lindquist NL, Martens CS (2018) Consumption of dissolved organic carbon by Caribbean reef sponges. *Limnol Oceanogr* 63:337–351
- Jackson JBC, Winston JE (1982) Ecology of cryptic coral reef communities. I. Distribution and abundance of major groups of encrusting organisms. *J Exp Mar Bio Ecol* 57:135–147
- Johnson C, Klumpp D, Field J, Bradbury R (1995) Carbon flux on coral reefs: effects of large shifts in community structure. *Mar Ecol Prog Ser* 126:123–143
- Kleypas JA, McManu JW, Mene LAB (1999) Environmental limits to coral reef development: Where do we draw the line? *Am Zool* 39:146–159
- Kornder NA, Cappelletto J, Mueller B, Zalm MJL, Martinez SJ, Vermeij MJA, Huisman J, de Goeij JM (2021) Implications of 2D versus 3D surveys to measure the abundance and composition of benthic coral reef communities. *Coral Reefs* 40:1137–1153
- Kornder NA, Esser Y, Stoupin D, Leys SP, Mueller B, Vermeij MJA, Huisman JA, de Goeij JM (2022) Sponges sneeze mucus to shed particulate waste from their seawater inlet pores. *Curr Biol* 32:3855–3861. <https://doi.org/10.1016/j.cub.2022.07.017>
- Kötter I (2002) *Feeding ecology of coral reef sponges*. University Bremen, Bremen
- Kuhl M, Cohen Y, Dalsgaard T, Jorgensen BB, Revsbech NP (1995) Microenvironment and photosynthesis of zooxanthellae in scleractinian corals studied with microsensors for O<sub>2</sub>, pH and light. *Mar Ecol Prog Ser* 117:159–172
- Long MH, Berg P, de Beer D, Ziemann JC (2013) In situ coral reef oxygen metabolism: an eddy correlation study. *PLoS One* 8:e58581
- Lowe RJ, Falter JL (2015) Oceanic forcing of coral reefs. *Ann Rev Mar Sci* 7:43–66
- Maldonado M (2016) Sponge waste that fuels marine oligotrophic food webs: a re-assessment of its origin and nature. *Mar Ecol* 37:477–491
- Maldonado M, Ribes M, van Duyl FC (2012) Nutrient fluxes through sponges. *Advances in sponge science: physiology, chemical and microbial diversity, biotechnology*. Elsevier, pp 113–182. <https://doi.org/10.1016/B978-0-12-394283-8.00003-5>
- Mayer FW, Wild C (2010) Coral mucus release and following particle trapping contribute to rapid nutrient recycling in a Northern Red Sea fringing reef. *Mar Freshw Res* 61:1006–1014
- McMurray SE, Stubler AD, Erwin PM, Finelli CM, Pawlik JR (2018) A test of the sponge-loop hypothesis for emergent Caribbean reef sponges. *Mar Ecol Prog Ser* 588:1–14
- Nadon MO, Stirling G (2006) Field and simulation analyses of visual methods for sampling coral cover. *Coral Reefs* 25:177–185
- Naumann MS, Niggel W, Laforsch C, Glaser C, Wild C (2009) Coral surface area quantification-evaluation of established techniques by comparison with computer tomography. *Coral Reefs* 28:109–117
- Naumann MS, Haas A, Struck U, Mayr C, El-Zibdah M, Wild C (2010) Organic matter release by dominant hermatypic corals of the Northern Red Sea. *Coral Reefs* 29:649–659
- Naumann MS, Richter C, Mott C, El-Zibdah M, Manasrah R, Wild C (2012) Budget of coral-derived organic carbon in a fringing coral reef of the Gulf of Aqaba, Red Sea. *J Mar Syst* 105–108:20–29
- Niquil N, Jackson GA, Legendre L, Delesalle B (1998) Inverse model analysis of the planktonic food web of Takapoto Atoll (French Polynesia). *Mar Ecol Prog Ser* 165:17–29

- Odum HT, Odum EP (1955) trophic structure and productivity of a windward coral reef community on eniwetok atoll. *Ecol Monogr* 25:291–320
- Olinger LK, Strangman WK, McMurray SE, Pawlik JR (2021) Sponges with microbial symbionts transform dissolved organic matter and take up organohalides. *Front Mar Sci* 8:665789
- Pawlik JR, McMurray SE (2020) The emerging ecological and biogeochemical importance of sponges on coral reefs. *Ann Rev Mar Sci* 12:315–337
- Rädecker N, Meyer FW, Bednarz VN, Cardini U, Wild C (2014) Ocean acidification rapidly reduces dinitrogen fixation associated with the hermatypic coral *Seriatopora hystrix*. *Mar Ecol Prog Ser* 511:297–302
- Rasheed M, Al-Trabeen K, Badran M (2012) Long-term water quality monitoring at an industrial site on the Northern Gulf of Aqaba, Red Sea. *Mediterr Mar Sci* 13:250–258
- Reidenbach MA, Monismith SG, Koseff JR, Yahel G, Genin A (2006) Boundary layer turbulence and flow structure over a fringing coral reef. *Limnol Oceanogr* 51:1956–1958
- Richter C, Wunsch M, Rasheed M, Kötter I, Badran MI (2001) Endoscopic exploration of Red Sea coral reefs reveals dense populations of cavity-dwelling sponges. *Nature* 413:726–730
- Rix L, de Goeij JM, Mueller CE, Struck U, Middelburg JJ, van Duyl FC, Al-Horani FA, Wild C, Naumann MS, Van Oevelen D (2016) Coral mucus fuels the sponge loop in warm-and cold-water coral reef ecosystems. *Sci Rep* 6:1–11
- Rix L, de Goeij JM, van Oevelen D, Struck U, Al-Horani FA, Wild C, Naumann MS (2017) Differential recycling of coral and algal dissolved organic matter via the sponge loop. *Funct Ecol* 31:788
- Rix L, de Goeij JM, Van Oevelen D, Struck U, Al-Horani FA, Wild C, Naumann MS (2018) Reef sponges facilitate the transfer of coral-derived organic matter to their associated fauna via the sponge loop. *Mar Ecol Prog Ser* 589:85–96
- Roth F, Radecker N, Carvalho S, Duarte CM, Saderne V, Anton A, Silva L, Calleja ML, Morán XAG, Voolstra CR, Kürten B, Jones BH, Wild C (2021) High summer temperatures amplify functional differences between coral- and algae-dominated reef communities. *Ecology* 102:e03226
- Santos HF, Carmo FL, Duarte G, Dini-Andreote F, Castro CB, Rosado AS, Van Elsas JD, Peixoto RS (2014) Climate change affects key nitrogen-fixing bacterial populations on coral reefs. *ISME J* 8:2272–2279
- Schrammeyer V, Wangpraseurt D, Hill R, Kühl M, Larkum AWD, Ralph PJ (2014) Light respiratory processes and gross photosynthesis in two scleractinian corals. *PLoS One* 9:e110814
- Shashar N, Kinane S, Jokiel PL, Patterson MR (1996) Hydromechanical boundary layers over a coral reef. *J Exp Mar Bio Ecol* 199:17–28
- Silverman J, Lazar B, Erez J (2007) Community metabolism of a coral reef exposed to naturally varying dissolved inorganic nutrient loads. *Biogeochemistry* 84:67–72
- Sing Wong A, Vrontos S, Taylor ML (2022) An assessment of people living by coral reefs over space and time. *Glob Chang Biol* 28:7139–7153
- Soetaert K, van Oevelen D (2009) Modeling food web interactions in benthic deep-sea ecosystems: a practical guide. *Oceanography* 22(1):128–143. <https://doi.org/10.5670/oceanog.2009.13>
- Tilstra A, van Hoytema N, Cardini U, Bednarz VN, Rix L, Naumann MS, Al-Horani FA, Wild C (2018) Effects of water column mixing and stratification on planktonic primary production and dinitrogen fixation on a northern red sea coral reef. *Front Microbiol*. <https://doi.org/10.3389/fmicb.2018.02351>
- Tsehaye I, Nagelkerke LAJ (2008) Exploring optimal fishing scenarios for the multispecies artisanal fisheries of Eritrea using a trophic model. *Ecol Modell* 212(3–4):319–333. <https://doi.org/10.1016/j.ecolmodel.2007.10.044>
- van Duyl FC, Gast GJ (2001) Linkage of small-scale spatial variations in DOC, inorganic nutrients and bacterioplankton growth with different coral reef water types. *Aquat Microb Ecol* 24:17–26
- van Duyl FC, Scheffers SR, Thomas FIM, Driscoll M (2006) The effect of water exchange on bacterioplankton depletion and inorganic nutrient dynamics in coral reef cavities. *Coral Reefs* 25:23–26
- van Hoytema N, Bednarz VN, Cardini U, Naumann MS, Al-Horani FA, Wild C (2016) The influence of seasonality on benthic primary production in a Red Sea coral reef. *Mar Biol* 163:1–14
- Varkey D, Ainsworth CH, Pitcher TJ (2012) Modelling reef fish population responses to fisheries restrictions in marine protected areas in the coral triangle. *J Mar Biol* 2012:1–18
- Vézina AF, Pahlow M (2003) Reconstruction of ecosystem flows using inverse methods: How well do they work? *J Marine Syst* 40–41:55–77. [https://doi.org/10.1016/S0924-7963\(03\)00013-7](https://doi.org/10.1016/S0924-7963(03)00013-7)
- Vézina AF, Platt T (1988) Food web dynamics in the ocean. 1. Best-estimates of flow networks using inverse methods. *Marine Ecol Progr Ser Oldendorf* 42(3):269–287
- Vicente J, Webb MK, Paulay G, Rakchai W, Timmers MA, Jury CP, Bahr K, Toonen R J (2021) Unveiling hidden sponge biodiversity within the Hawaiian reef cryptofauna. *Coral Reefs* 41(3):727–742. <https://doi.org/10.1007/s00338-021-02109-7>
- Webb KL, DuPaul WD, Wiebe W, Sottile W, Johannes RE (1975) Enewetak (Eniwetok) Atoll: aspects of the nitrogen cycle on a coral reef I. *Limnol Oceanogr* 20(2):198–210. <https://doi.org/10.4319/lo.1975.20.2.0198>
- Wild C, Huettel M, Klueter A, Kremb SG, Rasheed MYM, Jørgensen BB (2004) Coral mucus functions as an energy carrier and particle trap in the reef ecosystem. *Nature* 428(6978):66–70. <https://doi.org/10.1038/nature02344>
- Wooster MK, McMurray SE, Pawlik JR, Morán XAG, Berumen ML (2019) Feeding and respiration by giant barrel sponges across a gradient of food abundance in the Red Sea. *Limnol Oceanogr* 64(4):1790–1801. <https://doi.org/10.1002/lno.11151>
- Wunsch M, Al-Moghrabi SM, Kötter I (2000) Communities of coral reef cavities in Jordan, Gulf of Aqaba (Red Sea). In *Proc 9th Int Coral Reef Symp* 1
- Yahel G, Sharp JH, Marie D, Häse C, Genin A (2003) In situ feeding and element removal in the symbiont-bearing sponge *Theonella swinhoei*: bulk DOC is the major source for carbon. *Limnol Oceanogr* 48(1):141–149. <https://doi.org/10.4319/lo.2003.48.1.0141>
- Yahel G, Zalogin T, Yahel R, Genin A (2006) Phytoplankton grazing by epi- and infauna inhabiting exposed rocks in coral reefs. *Coral Reefs* 25:153–163

**Publisher's Note** Springer Nature remains neutral with regard to jurisdictional claims in published maps and institutional affiliations.